Journal of Atmospheric Chemistry **13**: 393–406, 1991.

Diffuse Radiation, Twilight, and Photochemistry – II

D. J. LARY and J. A. PYLE
Department of Chemistry, University of Cambridge, Cambridge CB2 1EW, U.K.

(Received: 9 July 1991)

Abstract. A photochemical scheme including a detailed description of multiple scattering up to solar zenith angles of 96° has been used to study a number of different datasets. The good agreement of the model with these datasets and the improvement over previous intercomparisons emphasise the importance of both the diffuse radiation field at wavelengths below 310 nm and multiple scattering at solar zenith angles greater than 90°. These features are ignored in some photochemical models but prove to be very important in modelling photochemistry at dawn and dusk.

Key words: Multiple scattering.

1. Introduction

In a companion paper, Lary and Pyle (1991) have described a radiation scheme which has been developed for use in atmospheric photochemical models. The scheme is based on Meier *et al.* (1982) and Anderson (1983). It includes the effects of ground reflection and a detailed treatment of multiple scattering up to a solar zenith angle of 96°. As such, it is particularly appropriate for the study of photochemical phenomena at dawn and dusk, as well as in polar latitudes. In the earlier paper a number of general features were discussed, in particular, the contrasting behaviour of diffuse radiation at wavelengths above and below 310 nm. Multiple scattering in the latter region is often not considered when calculating photolysis rates. The effect on the partitioning between the radical families was described in detail, as well as the impact on the calculated ozone in the model. Throughout, the role of diffuse radiation was emphasised and the importance of an accurate treatment of multiple scattering at wavelengths less than 310 nm was stressed.

In this paper we consider the scheme in detail, examining a number of cases where either the radiative transfer model can be validated or where the use of the model allows data to be interpreted in greater detail. We consider a number of specific cases. These include the radiative flux measurements of Herman and Mentall (1982), which allows the model to be validated; balloon and satellite measurements of the diurnal variation of nitrogen oxides, which provide a good test of the model treatment of the dawn and dusk transitions; and the ground based ultraviolet measurements of Lubin *et al.* (1989). These are now described in turn.

2. Comparison with Stratospheric Ultraviolet Measurments

A good test of any radiation model is, of course, the measured radiation field as a function of wavelength. Herman and Mentall (1982) made such measurements from a balloon at a float altitude of 40 km and a solar zenith angle of 41.2°. Two separate systems were used, one pointed directly at the sun, and the other oriented in six different directions away from the sun to determine the amount of scattered solar flux (Figure 1).

The scattered flux within the atmosphere can be estimated by integrating the measured specific fluxes over 4π steradians. Herman and Mentall measured specific fluxes in one plane in six specific directions (Figure 1). To do the integration they performed logarithmic interpolation between adjacent pairs of measurements. In addition they assumed that the specific flux in the direction of the sun is at least as large as F_6 (the flux from direction 6 measured by Herman and Mentall) in Figure 1. As pointed out by Herman and Mentall, since the maximum scattered flux is assumed to be F_6, the resulting integration is an underestimate of the total scattered flux. This is found to be the case (compare the Herman and Mentall data in Figure 2 with the model results). In an attempt to quantify the underestimate resulting from the assumption that F_6 was the maximum flux, the scattered flux in the numerical model was reduced by 80% (dashed curve in Figure 2). It can be seen that this produces much better agreement with the data between 210 and 300 nm.

The earlier theoretical work of Luther and Gelinas (1976) considered the flux ratio at 40 km for a solar zenith angle of 60°, and a range of ground albedos. Their study reproduces the contribution from diffuse flux for $\lambda > 300$ nm, but shows no contribution from diffuse flux for $\lambda < 210$ nm, contrary to the measurements of Herman and Mentall (1982). R. J. Gelinas pointed out that this is probably due to the bin-averaged cross sections used in the Schumann–Runge bands of oxygen

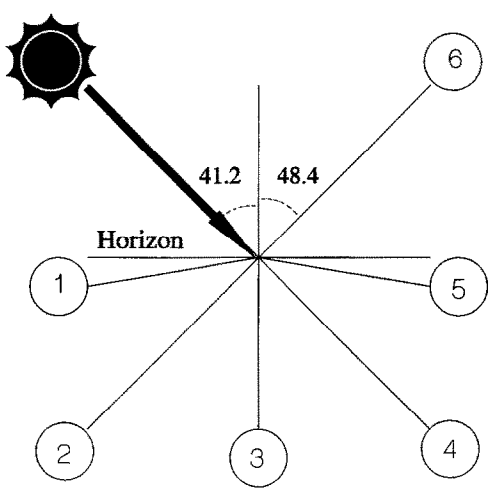

Fig. 1. The measurement geometry used by Herman and Mentall (1982).

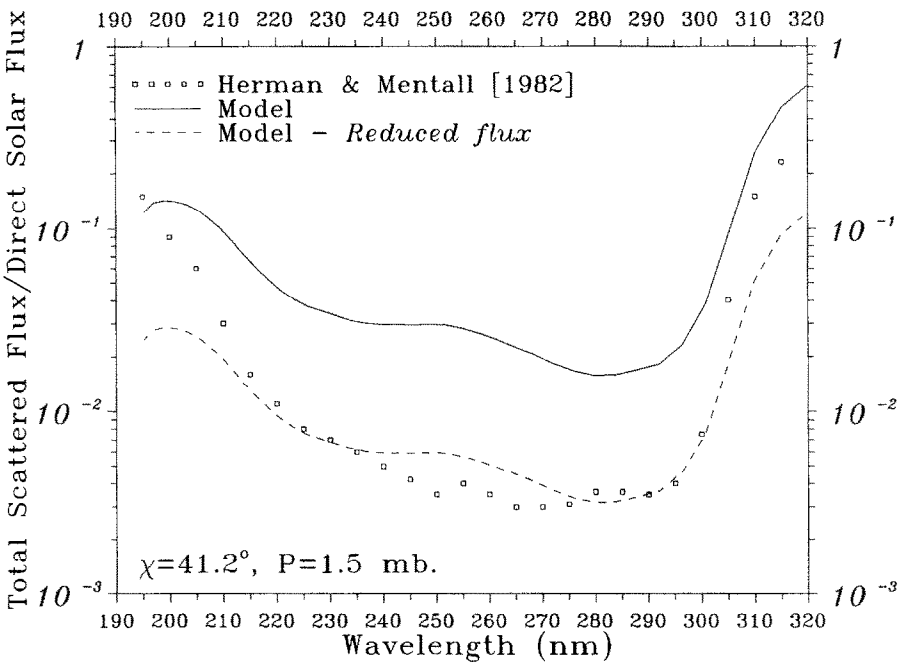

Fig. 2. The diffuse to direct solar flux ratio at 40 km for a solar zenith angle of 41.2°, estimate from measurements (squares) and calculated (lines)

(private communication to Herman and Mentall (1982). This study uses the parameterisation of Frederick (1985) to calculate the absorption cross section for the Schumann–Runge bands of molecular oxygen.

Notice that the ratio is very wavelength dependent, becoming larger at wavelengths greater than 300 nm and in the ultraviolet window at around 200 nm. The models has been run using a standard atmosphere ozone profile to calculate the ratio of scattered to direct flux at 40 km and a zenith angle of 41.2°, the conditions of the Hermann and Mentall (1982) measurements. Figure 2 shows that the wavelength dependence of the ratio is well reproduced by the model.

Two conclusions can be drawn from the example. Firstly the model appears to be validated by the measurements. Secondly, there is clearly an important role played by the scattered radiation at wavelengths below 300 nm. In particular, the contribution to photolysis by diffuse radiation in the important window region around 200 nm is certainly not negligible and should be included in photolysis rate calculations.

Notice that the increase in the photolysis rate of O_2 due to diffuse radiation at these wavelengths is an important source of O_3 (see Lary and Pyle (1991), Figure 2).

3. The Diurnal Variation of NO and NO_2

3.1. *Balloon Measurements*

Nitric oxide is one of the few photochemically active gases for which there are measurements with a high time resolution. In the sunlit stratosphere, NO is in immediate photochemical equilibrium with NO_2. The reactions which give rise to the rapid $NO_x = (NO + NO_2)$ interchange are listed in Table I. If NO_2 is in photochemical equilibrium then $d[NO_2]/dt = 0$, and the [NO] to $[NO_2]$ ratio can be written as

$$\frac{[NO]}{[NO_2]} = \frac{k_3[O] + jNO_2}{k_1[O_3] + k_2[ClO] + k_4[HO_2]}. \tag{1}$$

jNO_2 is a major term in this expression, and high time resolution measurements of NO are an ideal test for appraising the accuracy of a photochemical radiative transfer model.

Measurements of NO at sunset were made by Kondo *et al.* (1985, 1988) using a balloon borne chemiluminescent instrument flown from Aire sur l'Adour. The data were considered by Roscoe and Pyle (1987) who were unable to match precisely the zenith angle variation with their numerical model. Figure 3 shows results from their paper. A photolysis scheme including no treatment of Rayleigh scattering failed badly to reproduce the data. When the effect of Rayleight attenuation of the direct beam was considered the agreement between model and data was improved, but the model still calculates too large an NO concentration at high solar zenith angles.

Figure 4 shows a comparison between measured NO and model calculations using the present radiation scheme. Agreement between model and data is excellent. It is clear that an accurate description of multiple scattering during twilight is necessary to reproduce the details of the diurnal variation of short lived species such as NO at dawn and dusk.

3.2. *Satellite Measurements*

Polar orbiting satellites on a sun-synchronous orbit always cross the equator at the same local time. However, the measurements made in high latitudes cover a wide

Table I.

	$NO + O_3$	$\rightarrow$ $NO_2 + O_2$	(1)	
	$NO + ClO$	$\rightarrow$ $NO_2 + Cl$	(2)	
	$NO_2 + O$	$\rightarrow$ $NO + O_2$	(3)	
	$NO + HO_2$	$\rightarrow$ $NO_2 + OH$	(4)	
$\lambda > 410$ nm	$NO_2 + h\nu$	$\rightarrow$ $NO + O$	(5)	jNO_2
	$NO_2 + O_3$	$\rightarrow$ $NO_3 + O_2$	(6)	
	$NO_2 + NO_3$	$\xrightarrow{M}$ N_2O_5	(7)	
	N_2O_5	$\xrightarrow{M}$ $NO_2 + NO_3$	(8)	

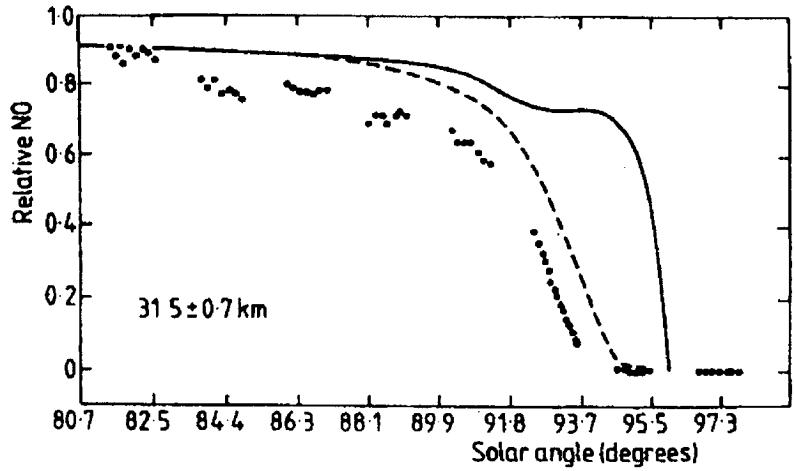

Fig. 3. Comparison of NO measurements made by Kondo *et al.* (1985) (points) with the model of Roscoe and Pyle (1987) (solid line) and the same model with improved Rayleigh scattering (dashed line).

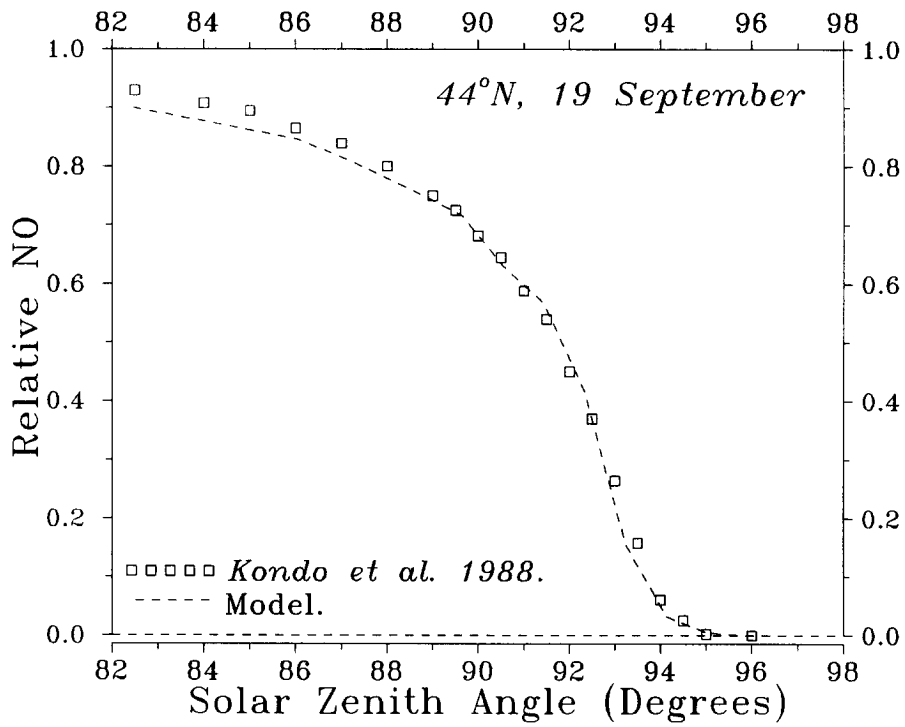

Fig. 4. Comparison of NO measurements made by Kondo *et al.* (1988) and model calculations including a detailed treatment of multiple scattering.

range of zenith angles, and therefore, local times from which diurnal variations can be constructed. Solomon *et al.* (1986) presented a similar reconstruction of the

NO_2 diurnal cycle (Figure 5) from LIMS. This was done by using the observations of NO_2 made between 56° N and 84° N, over the period 1 May to 28 May 1979. As a consequence of the dynamical stability over this period, the local variability in NO_2 caused by atmospheric motions was very small, and did not overwhelm the diurnal variation of NO_2.

The model calculations presented by Solomon *et al.* (1986) in Figure 5 are as follows: The dashed line is for a model assuming pure absorption and single scattering, while the solid line is for a model obtaining columnar multiple scattering with an albedo of 0.3.

The diurnal cycle reconstructed in this way is best termed a quasi-diurnal cycle, since, for at least four reasons, no 'real' diurnal cycle of NO_2 which occurred during May 1979 can simultaneously go through all the LIMS measurements. Firstly, no single May diurnal cycle spans the solar zenith angle range 34° to 109°. Secondly, the levels of NO_2 are sensitive to ozone, and there was a significant latitudinal gradient, and temporal change, of ozone during May. Thirdly, the levels of NO_2 are sensitive to temperature, and there was a temporal change in temperature during the month (albeit small). Fourthly, since the sun never sets poleward of approximately 70° N during May, whereas there is still a diurnal cycle equatorward of approximately 70° N, the partitioning of reactive nitrogen species will change with latitude (for example, in the region of constant illumination, photolysis will lead to much lower levels of N_2O_5).

This section compares the LIMS data with our photochemical model. Our analysis differs somewhat from that presented by Solomon *et al.* (1986). In particular, we consider each latitude band separately and consider variations which may have occurred during May. We will examine in detail the data at 68° N, where the diurnal variation was most pronounced.

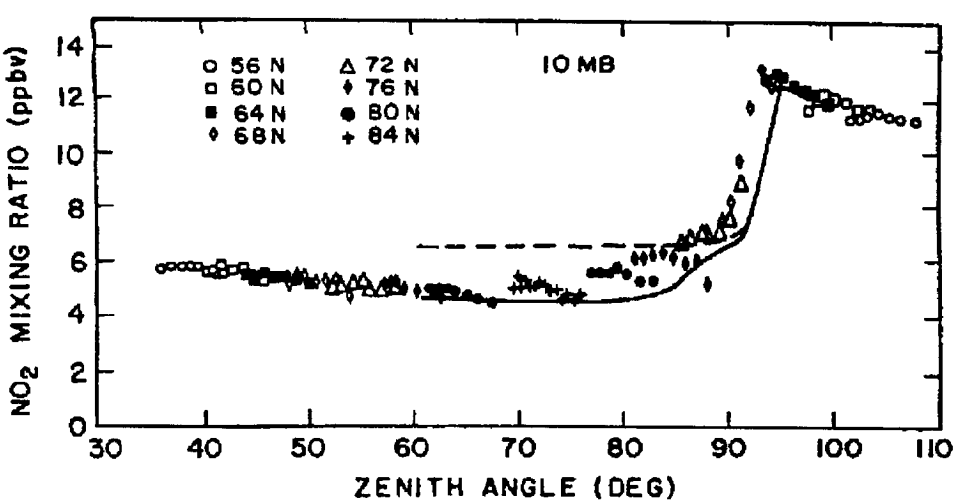

Fig. 5. Observed variation in NO_2 at 10 mb from 56° N to 84° N during May as a function of zenith angle, zonally and 4-day averaged (Solomon *et al.* (1986) fig. 2c).

A latitudinal gradient of ozone existed during May, with a monthly zonal mean of approximately 6.9 ppmv at 56° N decreasing to less than 5 ppmv at 84° N. For all latitudes there was also a temporal trend, with values at the end of May being approximately 10% less than at the beginning of the month (Solomon *et al.*, 1986). In this study, the zonal monthly mean ozone at 10 mb was found by applying a least squares fit to the LIMS and SBUV ozone data for May, given by Russell *et al.* (1986). If ϕ is the latitude in degrees between 56° N and 84° N, then the zonal monthly mean ozone concentration in ppmv is approximated by

$$(O_3)_{mean} = 11.08 - 0.075\phi. \quad (2)$$

The latitudinal temperature gradient was very small compared to that of ozone, and for any given day it did not exceed 4 K for the latitude band 56° N to 84° N, with the mean for this latitude band of approximately 234 K. There was a temporal temperature increase during the month of as much as 10–15 K (Solomon *et al.*, 1986).

This study assumed that, in accordance with the observations, there is a latitudinal gradient in the zonal mean ozone concentration given by Equation (2) and that there is a temporal change in ozone of 10% at all latitudes, i.e. ozone values on 1 May are 5% higher than given by Equation (2) and on 28 May are 5% lower than given by Equation (2). The reactive nitrogen content of the model was then adjusted for each latitude band in order to obtain a good agreement with the LIMS NO_2 data. The model was able to reproduce well the NO_2 measurements, as can be seen in Figures 6 and 7.

The agreement of the model with the LIMS measurements was improved when the rate constants for the OH reactions with HO_2 and H_2O_2 were taken from DeMore *et al.* (1990) instead of DeMore *et al.* (1987). This reflects the effect of OH concentrations on the levels of HO_2 and HNO_3, and hence the partitioning of reactive nitrogen.

The effect of the planet's changing solar illumination, and the temporal decrease in ozone levels during May, can be seen in Figure 6. Each plot contains two curves, one corresponding to a solar illumination at the start of May, with an ozone concentration 5% higher than is given by Equation (2) and the other corresponding to a solar illumination at the end of May, with an ozone concentration 5% lower than given by Equation (2). In each case, a model temperature of 234 K was used (i.e. close to the monthly mean for May 1979.

3.2.1. *56° N to 64° N.* Due to the seasonal evolution of the solar declination angle, the terminator retreats southward during May as the height of summer is approached. This is reflected in the LIMS measurements of NO_2. For example, in Figure 6 (a) and (b), if the nighttime decay of NO_2 is examined it is clear which measurements were taken at the beginning of May, and which ones were taken at the end of May. Those made at the start of the month can extend up to solar zenith angles of 109°, whereas at the end of May the maximum zenith angle had decreased

a) 56°N.

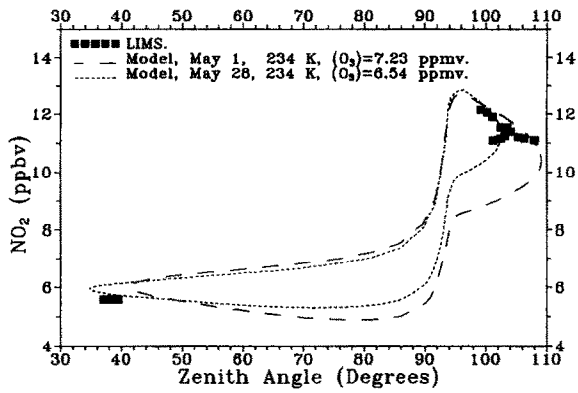

b) 60°N.

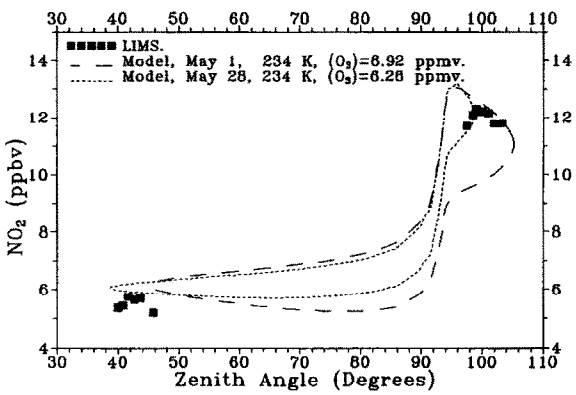

c) 64°N.

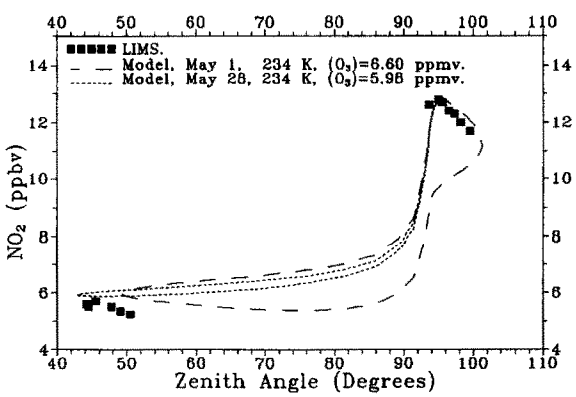

Fig. 6. A comparison of the diurnal variation of NO_2 at 10 mb observed by LIMS (squares) and simulated (line) for 56° N to 64° N during May 1979.

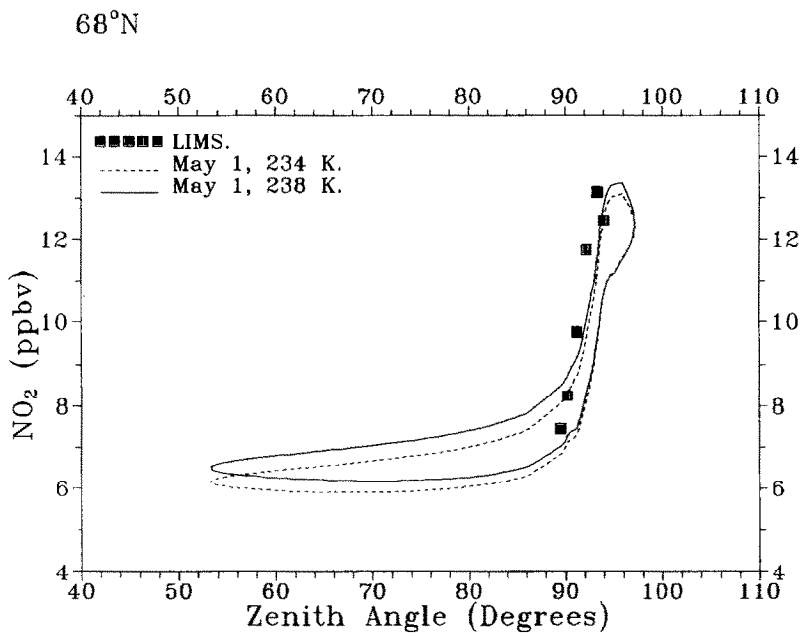

Fig. 7. A comparison of the diurnal variation of NO_2 at 10 mb observed by LIMS (squares) and simulated (line) for 68° N during May 1979.

to approximately 104°. In like manner, the measurements made at solar zenith angles close to 40° could only have been made at the end of May.

3.2.2. *68° N.* The two model calculations shown in Figure 7 are for a solar illumination corresponding to 1 May. The lower dotted curve is for an ozone concentration typical of early May and a temperature of 234 K, while the upper solid curve is for an ozone concentration typical of mid-May, and a temperature of 238 K. This latitude band is interesting since the LIMS observations captured the swift sunset increase in NO_2.

Examination of Figure 5 shows that there was a slight offset between the increase in the NO_2 measured by LIMS at solar zenith angles greater than 90° and those modelled by Solomon *et al.* (1986). While there are still discrepancies, the timing of the increase seems somewhat better in our calculations (Figure 7). The details of our respective treatments of scattering may be playing some role here. Figure 8 shows the effect of neglecting multiple scattering when calculatng the diurnal cycle of NO_2. It is interesting to note that the amplitude and shape of the NO_2 diurnal cycle are both affected by this approximation.

The comparison of calculated NO_x with observations of its diurnal variation provide a good test of the treatment of radiation in the model. In the cases considered, generally very good agreement has been found for both the case of in situ balloon observations and diurnal variations derived from satellite data.

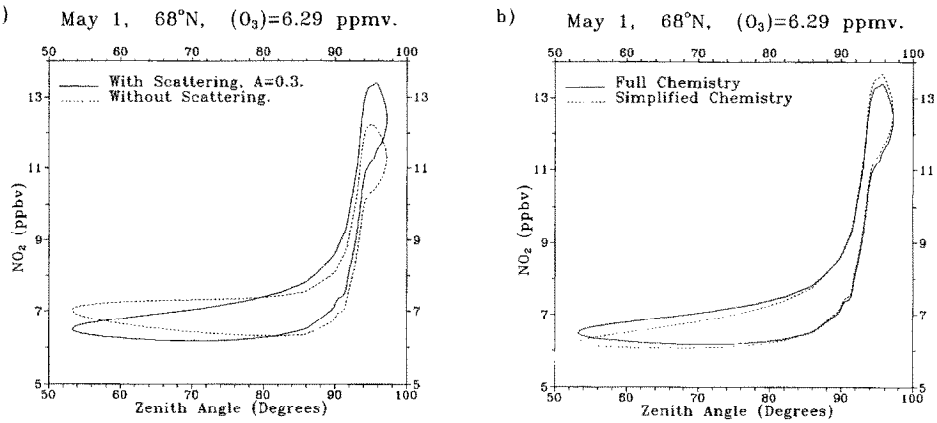

Fig. 8. The effect of ignoring multiple scattering on the calculated diurnal variation of NO_2 with $[O_3] = 6.29$ pp ppmv (see text for explanation).

4. Groundbased UV Measurements and Total Ozone

In the preceding two sections we have used observations of the ultraviolet radiation field to validate our treatment of diffuse radiation, and observations of NO and NO_2 to validate the performance of the radiation model at high solar zenith angles. In this final section we turn to ground based observations of ultraviolet radiation and use our model to interpret the data in terms of the total atmospheric ozone abundance.

The ozone absorption cross section decreases by two orders of magnitude from 295 nm to 330 nm. As a result, UV-B radiation (280 nm to 320 nm) is very sensitive to the total ozone column, whereas UV-A radiation (320 nm to 400 nm) is relatively insensitive to the total ozone column. Therefore, a good index of ozone depletion is the ratio of UV-B to UV-A irradiance at the earth's surface. Measurements of this ratio were made by Lubin *et al.* (1989) during the Austral spring of 1988. This study compares these measurements with model calculations.

During the Austral spring of 1988 two main factors gave rise to a change in the noontime irradiance ratio, a change in the noontime solar zenith angle resulting from the seasonal evolution of the solar declination, and a variation in the total ozone column. For a given wavelength, much of the measured UV variability was due to changing cloud cover. However, to a first approximation, the attenuation by clouds of both 300 nm and 340 nm is the same, and so the variability in the irradiance ratio $(I_{300\ nm})/(I_{340\ nm})$ due to changing cloud cover cancels out (Lubin *et al.*, 1989). Consequently the structure of the irradiance ratio is a reflection of the variation in total ozone. The vortex, which contains the region of maximum ozone depletion, is a dynamic entity and much of the observed variability in the irradiance ratio was caused by the vortex edge moving over Palmer Station.

Figure 9(a) shows irradiance ratios calculated using two models. One is the detailed radiative transfer model, while the other, Figure 9(b), contains no treat-

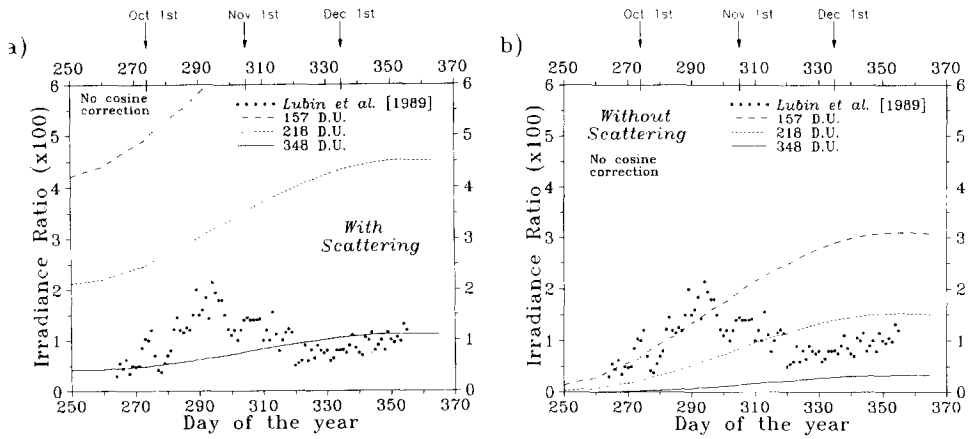

Fig. 9. Measurements of the UV-B/UV-A (×100) irradiance ratio at the earth's surface compared to model calculations made with; (a) the detailed radiative transfer model, and (b) no description of multiple scattering.

ment of scattering. In each case three different ozone profiles are used in the calculations. The first profile was the US Standard Atmosphere, with a total ozone content of 348 Dobson Units. This corresponds to a 'normal' atmosphere with no ozone depletion. The second profile was taken from the balloon sonde measurements made at Halley Bay (76° S, 27° W), on 26 September 1987 (Gardiner and Farman, 1988), with a total ozone content of 218 Dobson Units. The third profile was taken from the balloon sonde measurement made at Halley Bay on 13 October, 1987, and corresponds to one of the most severe ozone depletions on record, with a total ozone content of only 157 Dobson Units. To put these profiles into context, we note that the Antarctic ozone depletion was much less severe in 1988 than 1987. For example, the minimum values of the total ozone column recorded at Halley Bay during 1988 were only a little below 200 Dobson Units, with a mid-September to mid-October average of around 200 Dobson Units. There are very large differences between the model calculations made with and without a treatment of multiple scattering. The calculations made without including the effects of scattering can only be reconciled with the observations taken before mid-November if the ozone column was very low, significantly less than 200 Dobson Units. Indeed, an ozone hole deeper than that observed during 1987 would be required to explain the calculations which do not include multiple scattering. However, the ozone observations made during 1988 do not support this. On the other hand, the calculations including scattering do agree with the observations. When multiple scattering is considered it can be inferred from the measured irradiance ratio that the total ozone content did not go below approximately 200 Dobson Units and that the maximum irradiance ratio was seen just after the middle of October when the levels of total ozone were at their lowest. By the middle of November the irradiance ratio dropped close to the value calculated for a total ozone content of 350 Dobson Units, i.e. there was a relatively early recovery from the shallow 1988 'Ozone hole'.

Figure 10 shows the total ozone column above Palmer station which can be inferred from the measured irradiance ratio. A correction was made for the cosine response of the instrument so that a direct comparison could be made between the model and the measured irradiance ratio. Figure 10 also compares the inferred total ozone with the TOMS measurements for 1988 (These are the TOMS version 5 data, courtesy of the Geophysical Data Facility, Rutherfored Appleton Laboratory). Since the irradiance ratio measured by Lubin *et al.* (1989) was an instantaneous value (noon), Figure 10 also includes the minimum and maximum total ozone values observed by TOMS for 64° S.

The radiative transfer model which includes a description of multiple scattering (Figure 10(a)) is in good agreement with the TOMS measurements. However, it is interesting to note that the largest discrepancy is during October and early November (i.e. before day 300 when the noon time zenith angles are still rather large). This is in line with the concern that the TOMS version 5 dataset underestimates the total ozone column at large zenith angles (Lefèvre and Cariolle, 1991).

5. Conclusions

A photochemical scheme including a detailed description of multiple scattering up to solar zenith angles of 96° has been used to study a number of different datasets.

Measurements of the ultraviolet radiation field made by Hermann and Mentall (1982) agree well with the model. They emphasise the importance of the diffuse radiation field at wavelengths below 310 nm, ignored in some models.

Diurnal variation measurements provide a very good test of a radiative transfer model at high solar zenith angles. Comparison between two datasets have been described. The model agrees very well with the diurnal variation of NO as observed

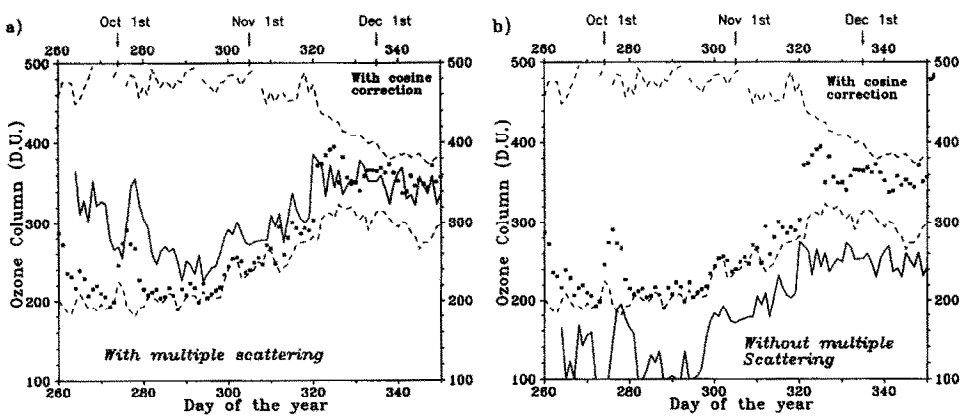

Fig. 10. TOMS Measurements of total ozone compared to the values of total ozone inferred from two sets of model calculations; (a) with multiple scattering, and (b) without multiple scattering. —— inferred ozone column, · · · · TOMS (64° S, 65° W), ------ TOMS min./max. for 64° S.

from a balloon borne instrument (Kondo *et al.*, 1985/1988). This is a marked improvement on earlier calculations (e.g. Roscoe and Pyle, 1987). Secondly, comparison with satellite measurements of NO_2 is also very good. Once again the high zenith angle transition is captured well, and appears to be better than that obtained in previous studies.

Finally, the model has been compared with the ground based ultraviolet measurements of Lubin *et al.* (1989). Calculations excluding the effects of scattering cannot explain these measurements, inferring a total ozone abundance which is much lower than was observed. On the other hand, the calculated irradiance ratio including multiple scattering agrees well with observations. The total ozone column inferred from these calculations compare well with the TOMS observations except at very high solar zenith angles where the accuracy of the TOMS version 5 dataset may be questioned.

In conclusion, these studies provide a very satisfactory validation of a powerful radiative transfer model for use in photochemical models. In particular, the treatment of diffuse radiation at wavelengths below 310 nm, and the inclusion of multiple scattering up to solar zenith angles of 96° are both extremely important components of the photochemical model.

Acknowledgements

D. Lary thanks SERC for a studentship, and H. K. Roscoe for many helpful discussions. The authors would like to thank the Geophysical Data Facility for granting access to its database. This work was supported by a CEC grant under STEP0013 for DGXII. This work forms part of the NERC U.K. Universities Global Atmospheric Modelling Programme.

References

Anderson, D. E., 1983, The troposphere to stratosphere radiation field at twilight: A spherical model, *Planet. Space Sci.* **31** (12), 1,517–1,523.

DeMore, W. B., Molina, M. J., Sander, S. P., Golden, D. M., Hampson, R. F., Kurylo, M. J., Howard, C. J., and Ravishankara, A. R., 1987, Chemical kinetics and photochemical data for use in stratospheric modelling, Evaluation Number 8, NASA JPL Publication 87-41.

DeMore, W. B., Molina, M. J., Sander, S. P., Golden, D. M., Hampson, R. F., Kurylo, M. J., Howard, C. J., and Ravishankara, A. R., 1990, Chemical kinetics and photochemical data for use in stratospheric modelling, Evaluation Number 9, NASA JPL Publication 90-1.

Frederick, J. E., 1985, The incident solar spectral irradiance and cross sections of molecular oxygen and ozone for use in the 1985 assessment report.

Gardiner, B. G. and Farman, J. C., 1988, Results of the 1987 ozonesonde programme at Halley Bay, Antarctica, British Antarctic Survey, Natural Environment Research Council, High Cross, Madingley Road, Cambridge CB3 0ET, U.K.

Goody, R. M., 1964, *Atmospheric Radiation: Theoretical Basis* (1st edn.), Oxford University Press, New York.

Herman, J. R. and Mentall, J. E., 1982, The direct and scattered solar flux within the stratosphere, *J. Geophys. Res.* **87**, 1,319–1,330.

Kondo, Y., Matthews, W. A., Iwata, A., and Takagi, M., 1985, Measurements of nitric oxide from 7 to

32 km and its diurnal variation in the stratosphere, *J. Geophys. Res.* **90**, 3,813–3,819.
Kondo, Y., Matthews, W. A., Aimedieu, P., and robbins, D. E., 1988, Diurnal variation of nitric oxide at 32 km: Measurements and interpretation, *J. Geophys. Res.* **93**, 2,451–2,460.
Kurzeja, R., 1976, Effects of diurnal variations and scattering on ozone in the stratosphere for present day and predicted future chlorine concentrations, *J. Atmos. Sci.* **34**, 1,120–1,129.
Lary, D. J., 1991, Photochemical studies with a three-dimensional model of the atmosphere, PhD Thesis, University of Cambridge, Cambridge, England.
Lary, D. J. and Pyle, J. A., 1991, Diffuse radiation, twilight, and photochemistry – I, *J. Atmos. Chem.* **13**, 373–392 (this issue).
Lefèvre, F. and Cariolle, D., 1991, Total ozone measurements and stratospheric cloud detection during the AASE and the TECHNOPS Arctic balloon campaign, *Geophys. Res. Lett.* **18**, 33–36.
Lubin, D., Frederick, J. E., Rocky Booth, C., Lucas, T., and Neuschuler, D., 1989, Measurements of enhanced spring time ultraviolet at Palmer station, Antarctica, *Geophys. Res. Lett.* **16**, 783–785.
Luther, F. M. and Gelinas, R. J., 1976, Effect of molecular multiple scattering and surface albedo on atmospheric photodissociation rates, *J. Geophys. Res.* **81**, 1,125–1,132.
Meier, R. R., Anderson, D. E., and Nicolet, M., 1982, The radiation field in the troposphere and stratosphere from 240 to 1000 nm: General analysis. *Planet. Space Sci.* **30**, 923–933.
Roscoe, H. K., and Pyle, J. A., 1987, Measurements of solar occultation: the error in a naive retrieval if the constituent concentration changes, *J. Atmos. Chem.* **5**, 323–341.
Russell, J. M. (ed.), 1986, Middle atmosphere program, *Handbook for MAP* **22**, SCOSTEP Secretariat, Illinois.
Solomon, S., Russell, J. M., and Gordley, L. L., 1986, Observations of the diurnal variation of nitrogen dioxide in the stratosphere, *J. Geophys. Res.* **91**, 5,455–5,464.